ANKARA BİLİM UNIVERSITY, RESEARCHER
Vol. 6, No. 1, July 2026
e-ISSN: 2717-9494
Research Article/Araştırma Makalesi

Linear Buckling Optimisation of Composite Plate in UAV Wing with Multi Objective Genetic Algorithm

Mehmet Ali GÜVENÇ[1*], Erkan KARAMAN[2], Hakan ÇAKMAK[3]
[1] Iskenderun Technical University, Faculty of Aeronautics and Astronautics, Department of Aerospace Engineering, İskenderun/Hatay, Türkiye ORCID: 0000-0002-4652-3048
[2] Iskenderun Technical University, Faculty of Aeronautics and Astronautics, Department of Aerospace Engineering, İskenderun/Hatay, Türkiye ORCID: 0009-0000-4247-3779
[3] Iskenderun Technical University, Faculty of Aeronautics and Astronautics, Department of Aerospace Engineering, İskenderun/Hatay, Türkiye ORCID: 0009-0006-1000-1201
*Corresponding Author: mali.guvenc@iste.edu.tr

Received: 27 May 2025; Accepted: 23 December 2025

Reference/Atıf: M.A. Güvenç, E.K. Karaman, H. Çakmak, "Linear Buckling Optimisation of Composite Plate in UAV Wing with Multi Objective Genetic Algorithm", Researcher

Abstract

With the advancement of technology, materials and production methods in the unmanned aerial vehicle (UAV) sector have undergone significant evolution. During the early production of aircraft, low strength materials were commonly used as structural components. Considering the developments in today's aviation industry, it has been observed that production technologies have evolved into innovative methods such as composite materials, additive manufacturing and integrated structures. In this study, structural design and buckling analyses were performed for the surface of UAV wing using composite material. Optimization was performed to increase the buckling load and reduce the Equivalent Stress. Plate thickness, rib thickness and stiffener thickness were selected as parameters for optimization. Linear buckling and optimization were carried out for each defined parameter. Lower and upper limits were specified for the parameters. The study achieved optimal results for structural design and buckling analysis values using the Genetic Algorithm as the optimization method. The final structure optimized by Genetic Algorithm is compared with the initial structural design and buckling analysis results. The conducted buckling analyses were performed on a three-stiffener and two-rib plate. As a result of the study, the buckling load increased by 25% and the structural weight decreased by 3.46%.

Keywords: Buckling, Genetic algorithm, Optimization, Structural Analysis, UAV Wing

1. Introduction

The design of unmanned aerial vehicles (UAV) is constantly evolving due to new standards of performance and safety in the aviation industry. One of the most important parts of these design changes is the wing design of the aircraft. Aircraft wings are among the elements that determine aircraft performance by combining critical elements such as aerodynamic efficiency, strength and weight. With these factors, linear buckling optimization of UAV has become an important topic in the field of aerospace engineering.

Optimizing the buckling strength of the UAV wing has an important point in terms of both increasing aerodynamic stability and optimizing material usage[1].Elements such as stiffeners and ribs are important structural parts of the UAV wing. These parts have a significant impact on the structural stiffness and aerodynamic performance of the UAV wing.

In this study, the linear buckling optimization of the plate part of the UAV wing with ribs and stiffeners will be discussed. With the optimization, the design of structural elements will be improved [2]. This optimization aims to optimize the critical buckling resistance and the equivalent stress of the wing plate, taking into account the linear effects of material properties. This study will contribute to the investigation of the change in design according to the buckling effect in UAV design by providing both a theoretical and practical perspective. Thus, it will contribute to making the new UAV's to be produced more efficient and reliable.

This study investigates the optimization process using genetic algorithm to increase the buckling resistance of composite panels in the UAV wing and aims to increase the knowledge in this field. Buckling can vary depending on the size, hardness, thickness of the stiffeners used in the skin and even the thickness of the composite if composites are used. Figure 1 shows local buckling in the fuselage of an airplane.

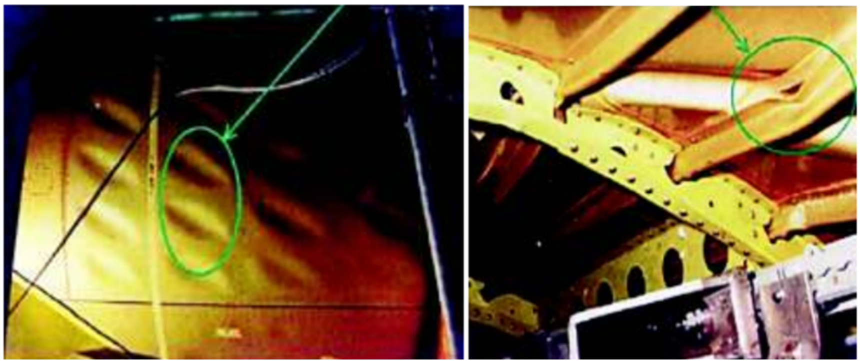

Figure 1: Local buckling of the airframe [3]

Usually, the plate part with stiffeners is made of aluminum materials. However, with the increase in the usage of composite materials in recent years, the aluminum coating structure has been replaced by composite materials. Another advantage of using composite materials in airplanes is that they can be used more easily in a maintenance and repair process on an aircraft, due to their lower cost in comparison. Composite structures are generally produced thin [4].

In their study, Kazemi et al. tried to increase the buckling strength of composite structures. In this section, they studied three optimizations to increase the buckling strength. The first is unrestricted optimization and the other two cases are constrained optimization subject to bending stiffness and elastic modulus constraints. A design for the maximal flexural stiffness and effective elastic module of the laminate has been developed to achieve the optimum orientation of the layers providing maximum flexural strength. As a general solution, they proposed the optimal stacking order of laminates. They determined the maximal value of the buckling load and the optimum layer angle for the output parameters [5].

Tekkanat, investigated a structural design for the use of wing-integrated reinforced panels on airplane wings. In this research, the same plate was subjected to buckling analysis using different types of stiffeners. As a result of the analysis, they obtained different force displacement graphs for each result. These results were compared for different types of stiffeners. They found that Panel B (panel with I type stiffener) and Panel D (panel with T type stiffener) had better buckling performance than the other panels. They concluded that Panel D (panel with T-type stiffener) can carry 50.1% more load than a plate design without stiffener [6].

Luca Lanzi et al. carried out a study on buckling optimization of composite reinforcing panels. They used a genetic algorithm and several different global optimization methods. These global optimization methods are Radial Basis Functions, Neural Networks and Kriging approach. The study discusses the challenges associated with the use and design of composite material in panels using stiffener. The authors investigated the post-buckling capacity and stability of the panels. They conducted tests to understand how these panels behave under load. They observed that the difference between calculations and tests was 5% [7].

The most important part that separates this study from other studies is the investigation of the composite plates of the wings of unmanned aerial vehicles. Otherwise, 2 ribs and 3 stiffeners were used in the study

[2] .The UAV plate was optimized with a genetic algorithm. This has given a new perspective to the research. This kind of study was not found in the literature review.

The panel used in this study was selected as "Epoxy Carbon Wowen", a composite material [8]. A verification study from previous studies was conducted to validate the study method. Linear buckling analysis of the first concept was performed. Then the desired values were optimized using the genetic algorithm.

2. MATERIALS AND METHODS

The block diagram given in Figure 2 models the progress of the study. The block diagram shows the stages of this study, starting with the creation of the stiffener panel geometry and ending with the optimization results. These stages are detailed in the following chapters.

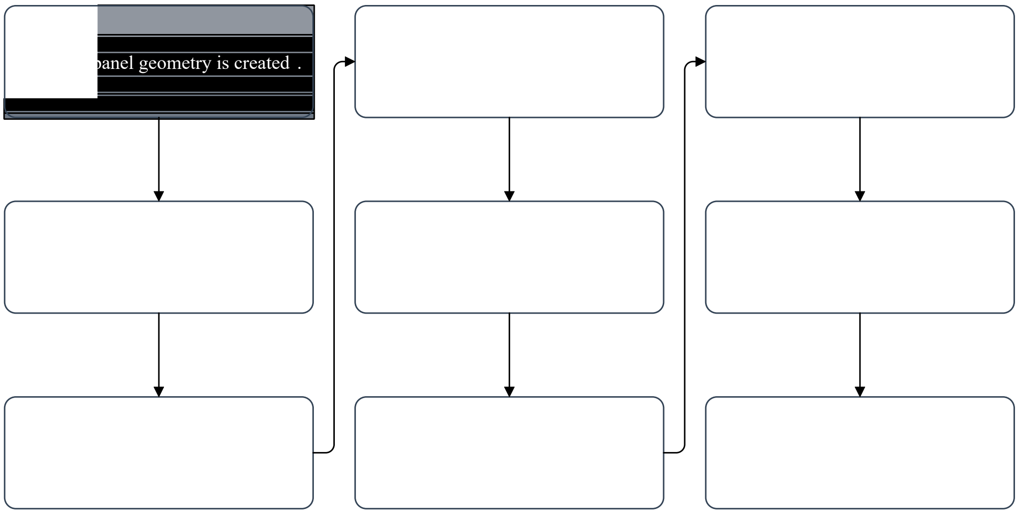

Figure 2: Block diagram in the study

1.1 Configurations of stiffened composite panel

In this study, a section of the wing plate is selected to be used in the buckling analyses. The geometrical properties of the section are shown in Figure 3. This geometry was made using SOLIDWORKS software. CAD drawings and dimensions of the section are shown in Figure 3. As shown in the figures, the wing plate structure has 3 stiffeners and 2 ribs.

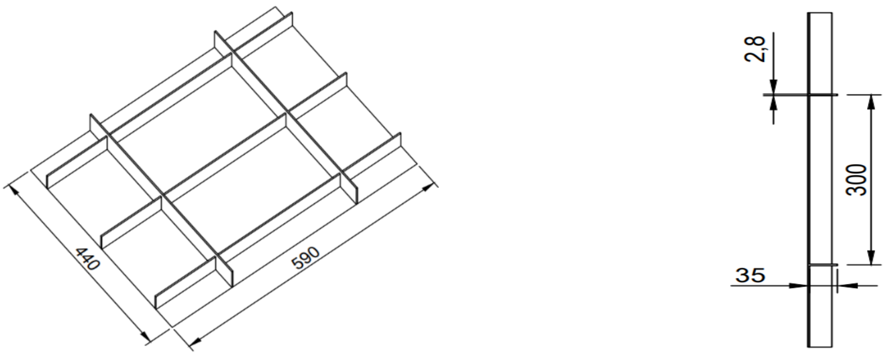

a) b)

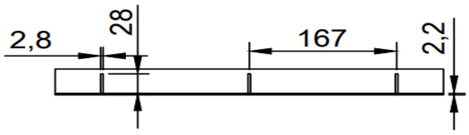

c)

Figure 3: Technical drawings of geometry a) Isometric view of geometry b) View of geometry from left c) Front view of geometry

2.2 Finite Element Model (FEM)

Finite element method was preferred in the analysis. The finite element method offers two methods for the prediction of linear buckling behavior. These are linear and nonlinear buckling analyses. The linear method is easier in calculation and the critical buckling load is obtained in the analyses. In nonlinear buckling analysis, buckling behavior is analyzed in longer times [9].The material and strength properties shown in Table 1 were used as materials. "Epoxy Carbon Wowen" was selected as the material [8]. The panel used in the study used a mesh size of 10 mm for better measurement of stress and buckling. The total number of elements and nodes are 3391 and 10945 respectively.

Table 1: Properties of Composite Materials

Material Properties	**Epoxy Carbon Woven (395 GPa) Prepreg**
Density	1480 km/mm^3
Modulus of Elasticity X Direction	91.82 GPa
Modulus of Elasticity Y Direction	91.82 GPa
Modulus of Elasticity Z Direction	9 GPa
Poisson's ratio XY	0.05
Poisson's ratio YZ	0.3
Poisson's ratio XZ	0.3
Shear Modulus XY	3.6 GPa
Shear Modulus YZ	3 GPa
Shear Modulus XZ	3 GPa
Tensile X Direction	0.829 GPa
Tensile Y Direction	0.829 GPa
Tensile Z Direction	0.05 GPa
Compression X Direction	-0.439 GPa
Compression Y Direction	-0.439 GPa
Compression Z Direction	-0.14 GPa
Shear X Direction	0.12 GPa
Shear Y Direction	0.05 GPa
Shear Z Direction	0.05 GPa

Boundary conditions were set to be compatible with linear buckling analyses. Structure boundary conditions for the panel used are shown in Figure 4. The bottom edge and top edge are prevented from moving in the Z axis. The upper and lower part is blocked from rotating in X and Z directions. The center point of the panel is blocked from moving in X and Y directions in order for buckling to occur and the center point to remain fixed in specific axes.

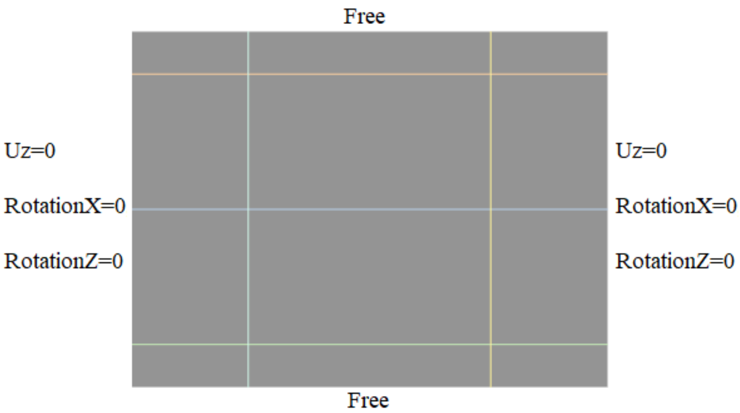

Figure 4: Boundary conditions for the analyses

At the end of the panel, a nodal point parallel to the center point in the X axis was determined and the movement of this point in the Y axis was prevented. This point can also be said as the parallel point of the center point. As shown in Figure 5, linear pressure was applied from the top and bottom edges of the plate [10] .

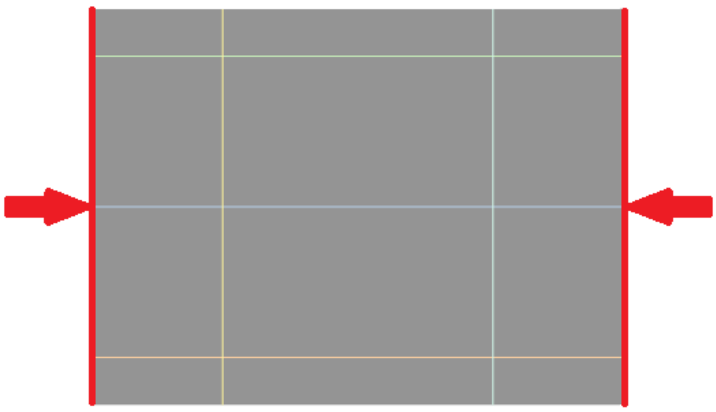

Figure 5: Showing the applied force directions for the analyses

The linear pressure applied on the plate is -100 N/m on the Y axis for the upper edge and 100N/m for the lower edge.

2.3 Formulation

Euler's minimum buckling force (F_{bk}) takes the value as shown in Formula 1 during buckling.

$$F_{bk} = \frac{\pi^2 \cdot E \cdot I}{L_{bk}^2} \quad (1)$$

Where;

E: Modulus of Elasticity (N/mm^2)

I: moment of inertia (mm^4)

L_{bk}: length of the column (mm)

$$\{u\} = \sum_{i=1}^{4} N_{m_i}\{u_i\} \tag{2}$$

$$\{v\} = \sum_{i=1}^{4} N_{m_i}\{v_i\} \tag{3}$$

$$\begin{Bmatrix} w \\ \theta_x \\ \theta_y \end{Bmatrix} = \sum_{i=1}^{4} N_{b_i} \begin{Bmatrix} w \\ \theta_x \\ \theta_y \end{Bmatrix}, i = 1, \dots, 4 \tag{4}$$

$$u(x, y, z) = u_0(x, y) - z\theta_{y,} \qquad \theta_y = \frac{\partial w_0}{\partial x} \tag{5}$$

$$v(x, y, z) = v_0(x, y) - z\theta_{x,} \qquad \theta_x = \frac{\partial w_0}{\partial x} \tag{6}$$

$$w(x, y, z) = w_0(x, y) \tag{7}$$

The expressions N_m and N_b in the equation are shape functions.Displacements in-plane and out-of-plane are as in the following equation.;

$$N_{m_i} = \frac{1}{4}\left[(1 + \xi_j\xi)(1 + \eta_j\eta)\right] \tag{8}$$

$$N_{b_i} = \frac{1}{8}[(1 + \xi_j\xi)(1 + \eta_j\eta)(2 + \xi_j\xi + \eta_j\eta - \xi^2 - \eta)$$
$$b(1 + \xi_j\xi)(\eta_j + \eta)(\eta^2 - 1)$$
$$-a(\xi_j + \xi)(\xi^2 - 1)(1 + \eta_j\eta)]$$
$$i, j = 1, .. ,4 \tag{9}$$

Where a, b, ε and η are the length, width and natural coordinates of the four-node rectangle, respectively. In Equation (9), the strain energy of the finite element is expressed as (U_e).

$$U_e = \frac{1}{2}\int_V \{\sigma\}_k^T \{\varepsilon\} dV \tag{10}$$

Here$\{\sigma\}^T$ is the matrix of stress components of the kth layer and $\{\epsilon\}$ is the strain matrix. The relationship between the stress tensor matrix and the material modulus matrix is given as $[Q]_k$.

$$\{\sigma\}_k^T = [Q]_k\{\varepsilon\} \tag{11}$$

or

$$\begin{bmatrix} \sigma_{xx} \\ \sigma_{yy} \\ \tau_{xy} \end{bmatrix} = \begin{bmatrix} Q_{11} & Q_{12} & Q_{16} \\ Q_{12} & Q_{22} & Q_{26} \\ Q_{16} & Q_{26} & Q_{66} \end{bmatrix}^k \begin{bmatrix} \varepsilon_{xx} \\ \varepsilon_{yy} \\ \gamma_{xy} \end{bmatrix}^k \tag{12}$$

The values of Q_{11}, Q_{12}, Q_{22}, Q_{16}, Q_{26} and Q_{66} in this matrix are obtained from the following equations. Where C=cosθ, s=sinθ. Composite layer angle is θ here [11], [12], [13].

$$Q_{11} = q_{11}c^4 + 2(q_{11} + 2q_{66})s^2c^2 + q_{22}s^4 \tag{13}$$

$$Q_{12} = (q_{11} + q_{22} - 4q_{66})s^2c^2 + q_{12}(s^4 + c^4) \tag{14}$$

$$Q_{22} = q_{11}s^4 + 2(q_{11} + 2q_{66}s^2c^2 + q_{22}c^4 \quad (15)$$

$$Q_{16} = (q_{11} - q_{12} - 2q_{66})sc^3 + (q_{12} - q_{22} + 2q_{66})s^3c \quad (16)$$

$$Q_{26} = (q_{11} - q_{12} - 2q_{66})s^3c + (q_{12} - q_{22} - 2q_{66})sc^3 \quad (17)$$

$$Q_{66} = (q_{11+}q_{12} - 2q_{12-}2q_{66})s^2c^2 + q_{66}(s^4 + c^4) \quad (18)$$

The material stiffness components $q_{ij}(i, j = 1,2,6)$ are calculated as in equations 19,20,21 and 22[13].

$$q_{11} = \frac{E_x}{1 - v_{xy}v_{yx}} \quad (19)$$

$$q_{12} = \frac{v_{xy}E_x}{1 - v_{xy}v_{yx}} \quad (20)$$

$$q_{22} = \frac{E_y}{1 - v_{xy}v_{yx}} \quad (21)$$

$$q_{66} = G_{xy} \quad (22)$$

D_{ij}, the bending stiffness matrix is calculated by the following equation [11], [12], [14].

$$D_{ij} = \begin{bmatrix} D_{11} & D_{12} & D_{16} \\ D_{12} & D_{22} & D_{26} \\ D_{16} & D_{26} & D_{66} \end{bmatrix} \quad (23)$$

$$D_{ij} = \frac{1}{3}\sum_{k=1}^{N}(Q_{ij})_k[{h_k}^3 - {h_{k-1}}^3] \quad (24)$$

In this equation Q_{ij} is obtained from the above equations. The $h_k$in the equation is the thickness of the (k) layer and $h_{k-1}$is the thickness of the number of (k-1) layer. After solving the matrix [13]

$$D_1 = D_{11} \quad (25)$$

$$D_2 = D_{22} \quad (26)$$

$$D_3 = D_{12} + D_{33} \quad (27)$$

D_1, D_2, D_3 Values are calculated. Then the buckling loading formula is as in Equation 10. Where a is the dimension of the long part of the plate and b is the dimension of the short part of the plate. The critical buckling load is obtained from the following formula.

$$N_{xcr} = \frac{-(\pi^2 \times a^2)}{c^2}\left[D_1\left(\frac{c}{a}\right)^4 + 2D_3\left(\frac{c}{a}\right)^2\left(\frac{s}{b}\right)^2 + D_2\left(\frac{s}{b}\right)^4\right] \quad (28)$$

2.4 Method validation

In this section, buckling analysis of a plate, which has been experimentally buckling analyzed, has been performed with analysis programs. The analyses performed on this plate were compared with the results of experimental buckling analyses. These analyses were performed to verify the methodology of the analyses to be performed in the study. CAD drawings showing the geometry and dimensions used for this validation study are given in Figure 6 [15].

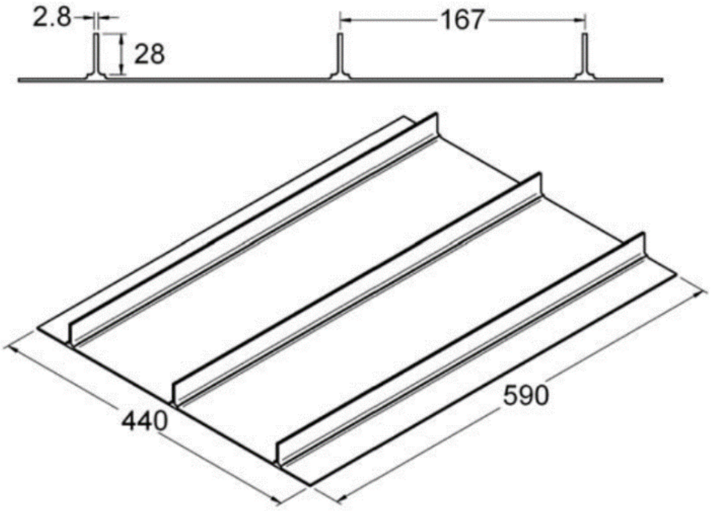

Figure 6. Geometry used by Quinn et al.

Aluminum 2024 T 351 alloy was used in this validation study. The properties of this aluminum alloy are given in Table 2 [15].

Table 2. Aluminum 2024 T 351 Material properties

	Density [kg/m^3]	Elastic Modulus [MPa]	Tensile Yield Strength [MPa]	Poisson Ratio	Ultimate Tensile Yield Strength [MPa]
Aluminum 2024 T 351	2780	73700	324	0.33	471

Analyses were carried out according to this material and the plate properties in the given CAD images and the results were listed and compared. These comparisons are shown below.

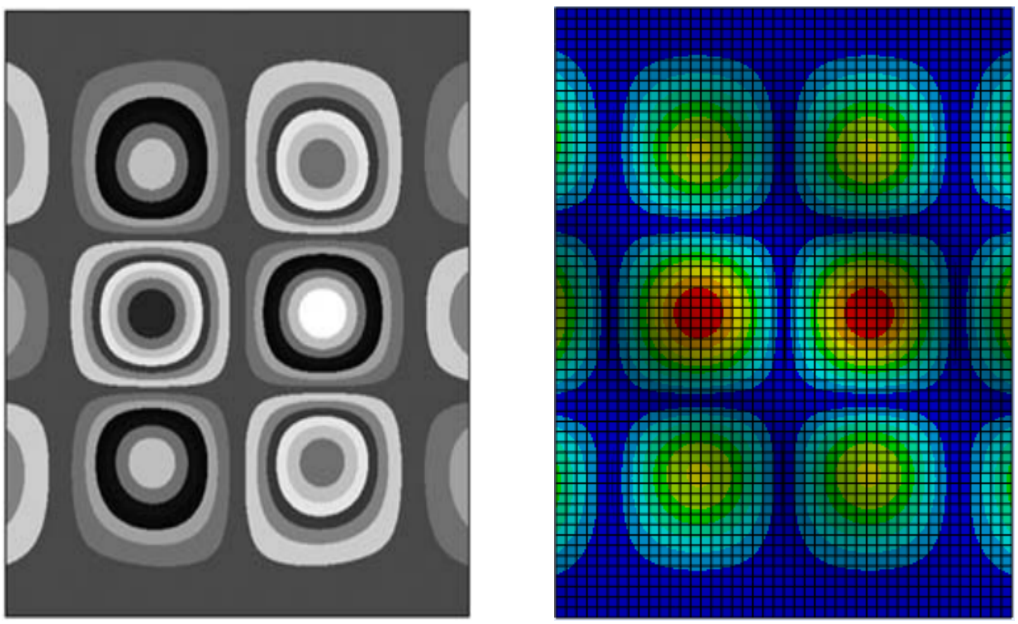

a) **b)**

Figure 7: Defects found as a result of research a) Eigen-mode defect [15] b) Defect found as a result of the analyses.

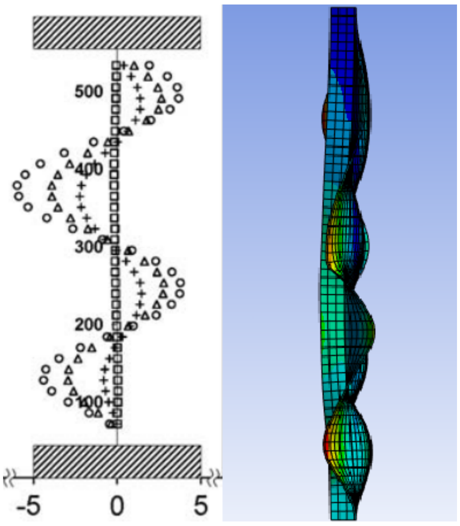

a) b)

Figure 8: Side view defect a) geometrical defects found by [15], b) geometrical defects found as a result of analyses

As shown in Figure 8, numerical results of our analysis and experimental results are presented. The results of the analyses made as a result of these comparisons coincide exactly with the experimental results [15]. In the verification study, the Total Deformation Load Multiplier value was obtained as 1357.3 N. The maximum equivalent stress value found was 1.8377 e-002 MPa. With this verification study, the method and process of the actual study to be carried out were verified.

2.5 Optimization

Like most situations, the most difficult part of making design is the definition of the structure. In general, the definition of design rules and the determination of appropriate configurations directly influence the design. For example, you could have increased one design requirement and decreased another design requirement. In fact, it is precisely in these cases that optimization is used. Optimization is the process of determining the best design. The best design of the problem is determined so as to achieve a given objective function by providing the available constraints [16], [17], [18].

In this part, the requirements of the composite plate with the determined input values and output values will be realized. Optimization is used in this case because of the multiple inputs and outputs. Optimization will be performed with Multi Objective Genetic Algorithm (MOGA).

Genetic Algorithm (GA) is a widely used method today. The goal of this algorithm is to find the optimal solution to the problem. When using a genetic algorithm, 4 main elements are identified. These elements are crossover, mutation, stopping criteria and selection. The aim of crossover is to produce new generations by moving the chromosome and to produce a new generation of chromosomes with high fitness values. Mutation is the alteration of some genes in selected chromosomes in order to increase the diversity among them.

If we talk about the advantages of change in the genetic algorithm, it prevents the research from entering a vicious circle with the help of mutation by providing changes in the direction of the solution area of the problem. Using GA, new generations are created to be better than previous generations. These generations continue to occur until the stopping criteria are met. There are several stopping criteria in this section. Such as mutation rate, population size or number of chromosomes [18], [19], [20]. Figure 9 shows the process of selectively replacing a gene from a chromosome.

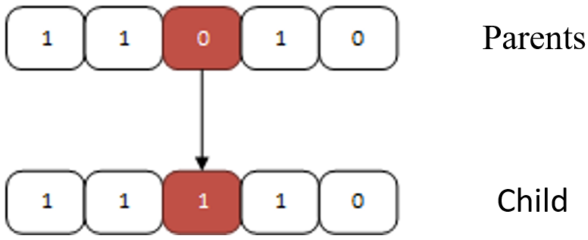

Figure 9*:* Selectively replacing a gene from a chromosome.

In this study, Multi Objective Genetic Algorithm and finite element method are combined to obtain the best solutions for the specified objective functions. In fact, this method is a modified version of the previous algorithm mentioned. In this method, the objective functions are directly recalculated by finite elements for each evaluation. In optimization, MOGA creates new parameters for each defined thickness. These parameters are then transferred to finite elements. It automatically performs many operations such as changing geometry with finite element software. The results including buckling load and equivalent stresses are transferred to MOGA. This process continues until the convergence criterion is met. Figure 10 shows the block diagram for the optimization [19], [21].

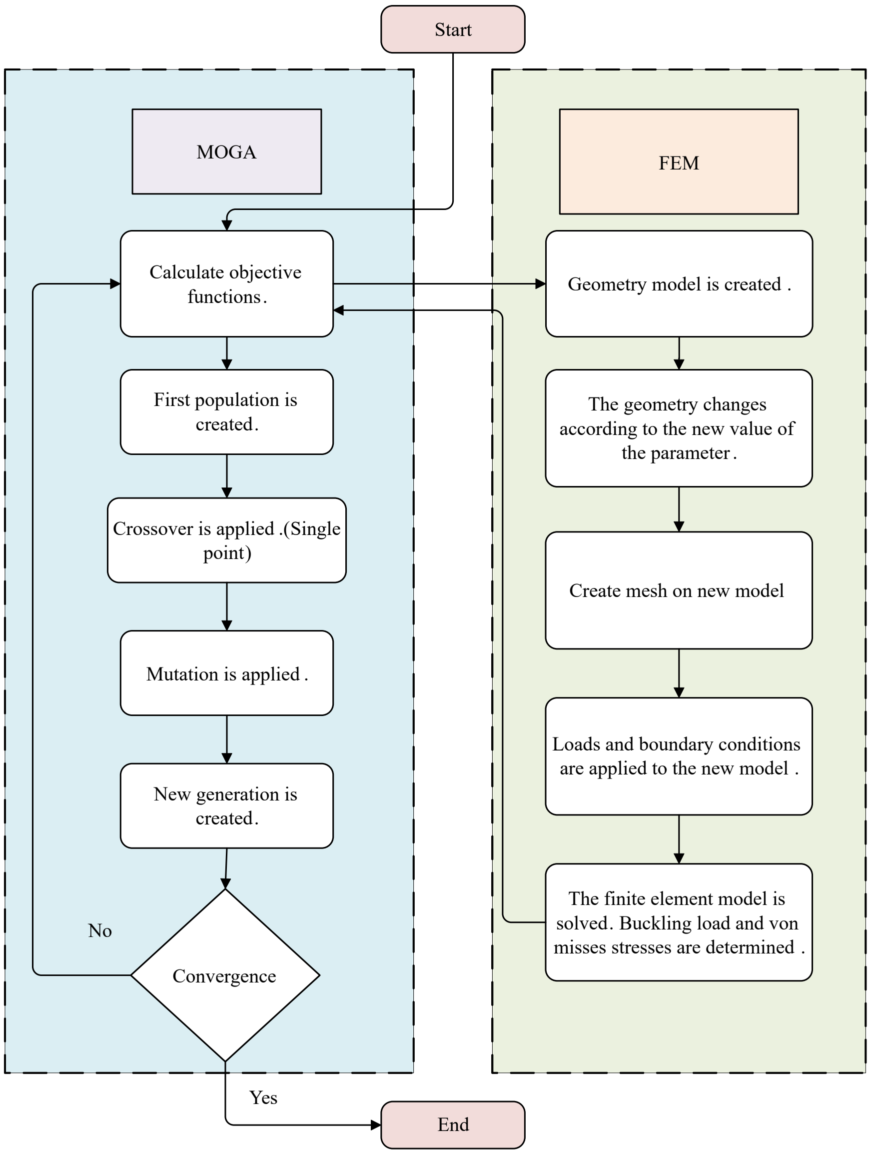

Figure 10: Optimization block diagram

2.5.1 Optimization Criteria:

The input parameters to be optimized are as follows. Lower and upper limits are entered for all input parameters. The upper and lower limits used in the optimization part are given in table 3 below.

t_1 = Middle Stiffener thickness

t_2 = Left Stiffener thickness

t_3 = Right Stiffener thickness

t_4 = Top Rib thickness

t_5 = Bottom Rib thickness

t_6 = Plate thickness

The desired output parameters in the optimization are as follows. The goal of this optimization is to minimize the point where the equivalent stress is maximum and maximize the initial buckling force.

$$F_1(x) = \min[\text{Equivalent Stress}]$$

$$F_2(x) = \max[\text{Buckling Load}]$$

3. Finding and Results

The geometry, boundary conditions and applied forces were analyzed. This section will present the results of this analysis and the optimized results together with the pre-optimization analysis results.

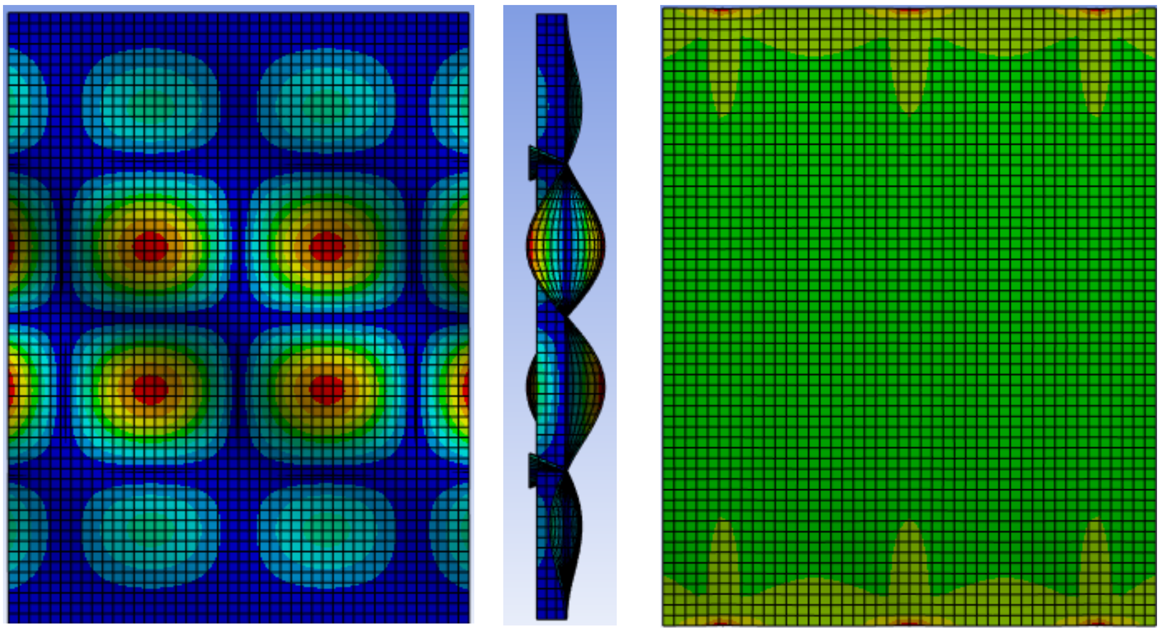

a) **b)** **c)**

Figure 11: Results of the research buckling analysis result of the design before optimization b) Geometric imperfection of the design before optimization c) Equivalent stress result found as a result of the analysis

Linear eigenvalue analysis was performed using ANSYS to find the initial buckling load. The first buckling mode obtained as a solution of the analysis is shown in Figure 11. As a result of buckling analysis of the structure, the load factor was found to be 811.05. This value is obtained by the ratio of the initial buckling load to the applied load. After multiplying the value obtained from the buckling analysis by the applied load, the initial buckling load was computed as 81105 N. Total Weight value was obtained as 1.1783 kg. As seen in Figure 12, it is observed that the maximum equivalent stress is 67384 Pa and the minimum equivalent stress is 29.64 Pa.

$$\text{Load factor} = \frac{\text{Initial buckling load}}{\text{Load applied}}$$

$$\text{Load factor} \times \text{Load applied} = \text{Initial buckling load } (811.05) \times (100\ \text{N}) = 81105\ \text{N}$$

After the initial design values were found, 15 design points were created through ANSYS. Within the framework of the determined parameters, lower and upper values were determined and ANSYS generated 15 design points. Separate analyses were performed for these design points. As a result of the analysis, total deformation loading coefficient values and equivalent stress values of each point were obtained. The analysis used 3 stiffeners and 2 latitudinal ribs. The generated thickness values are set to be the same between the stiffeners. The same applies to ribs. These values are presented in Table 4. As a solution to the analysis, the optimization phase was started.

Table 3. Values at Design Points

Plate Thickness (mm)	Stiffener Thickness(mm)	Rib Thickness (mm)	Maximum Equivalent Stress (Pa)	Total Deformation Load Multiplier
2.1	2.1	2.1	61421.8	654.93
1.2	2.1	2.1	165308	157.58
3.00	2.1	2.1	58595.52	1779.63
2.1	1.2	2.1	109119.4	615.94
2.1	3.00	2.1	81025.65	718.50
2.1	2.1	1.2	61420.51	642.92
2.1	2.1	3.00	61422.08	678.77
1.36	1.36	1.36	94229.67	182.15
2.83	1.36	1.36	87172.14	1448.70
1.36	2.83	1.36	163424.4	242.20
2.83	2.83	1.36	45600.68	1561.90
1.36	1.36	2.83	94232.10	202.95
2.83	1.36	2.83	87169.51	1478.97
1.36	2.83	2.83	163403.6	264.05
2.83	2.83	2.83	45602.37	1593.78

As mentioned in the optimization section, Multi objective genetic algorithm was used in the optimization and the thickness values of the reinforcing and latitudinal ribs were selected as input. The output was set to minimize the maximum equivalent stress value and maximize the total deformation load multiplier. As a result of the optimization, the thicknesses were determined for the most optimum result among the thickness values entered and the stress and loading coefficient values were found according to these results. The values found are listed in table 5.

Table 4. Values after optimization

Parameter	Value
Middle Stiffener thickness	1.6 mm

Left Stiffener thickness	1.6 mm
Right Stiffener thickness	1.6 mm
Top Rib thickness	1.4 mm
Bottom Rib thickness	1.4 mm
Plate thickness	2.4 mm
Maximum Equivalent Stress	10161.5 Pa
Total Deformation Load Multiplier	1014.06

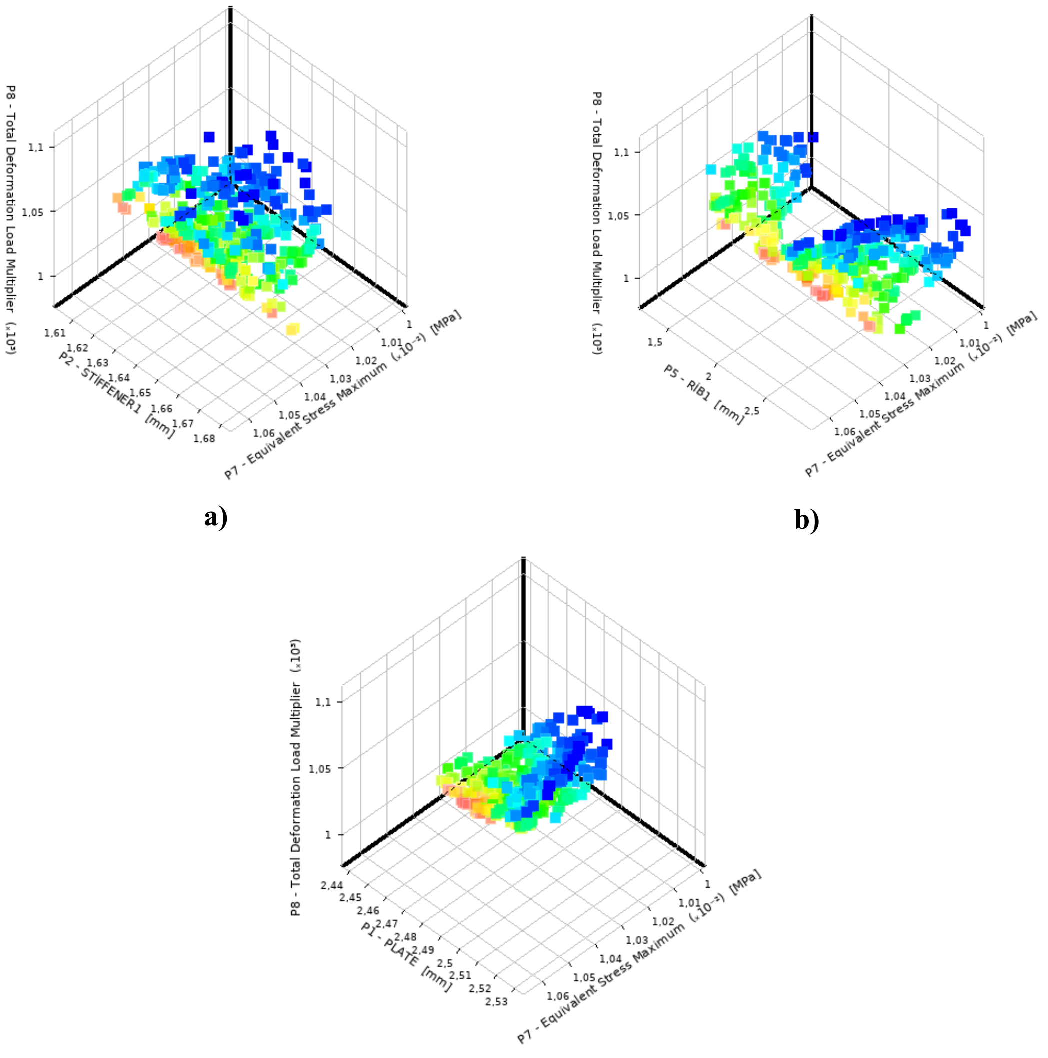

a) b) c)

Figure 12: Optimization Points a) optimization points for stiffener b) Optimization points for rib c)Optimization points for plate

As can be seen in Figure 12, the points tested for plate, stiffener and rib thicknesses respectively during the multi-objective genetic algorithm are shown as 3D tables. These tables also show the stress and loading coefficients for the thickness points tested. As a result of the optimization, the stiffener thicknesses were reduced from 2.8 mm to 1.6 mm and the rib thicknesses from 2.8 mm to 1.2 mm, and the plate thickness was increased from 2.2 mm to 2.4 mm within the given limits in order to minimize the maximum equivalent stress and maximize the total deformation loading multiplier. As a result, the equivalent stress value was reduced from

67.3 kPa to 10.1 kPa. Another output parameter, the total deformation loading multiplier, increased from 811.05 Nto 1014 N. As a result of the increase in this coefficient, the buckling load value increased from 81105 N to 101400 N.

As a result of optimization, our loading multiplier value increased significantly. This increase increased the minimum force that would cause buckling in the plate. In other words, the force at which the plate will start to buckle in the first analysis results was 101400 N while it was 81105 N. Looking at the maximum equivalent stress value, it is seen that there is a significant decrease compared to the first state.

4. Results

In this study, buckling analysis of the composite plate of an unmanned aerial vehicle wing with reinforcements is presented. Afterwards, an optimization was carried out with the genetic algorithm in a way to adhere to the lower and upper limits within the framework of the determined parameters.

After this optimization, the following results were obtained:

- There was a 25% increase in the total deformation loading multiplier value compared to the pre-optimization design. This increase increased the buckling load by 25%.
- The equivalent stress value decreased by 84.92% compared to the initial design.
- After optimization, the structural weight value decreased by 3.46%.

As a result of the optimization, the most effective parameter was found to be the plate thickness. The plate thickness increases while the thickness of the stiffeners and ribs decreases. Plate thickness increased by 9.09%.

5. Acknowledgements

We would like to thank Tübitak (Scientific and Technological Research Council of Turkey) for their support for our project numbered 1919B012317982 in the 2209-A University Students Research Projects Support Program.

6. References

[1] Ünler T, Dağ T, and Öztürk M, "Sabit Kanat Bir İnsansız Hava Aracı Konsept Tasarımı," in *3rd International Conference on Applied Engineering and Natural Sciences*, 2022.

[2] N. Yıldırım, S. Kurtar, G. Bedenli, and T. Dağ, "İNSANSIZ HAVA ARACI KANADINDA RİB SAYISINDAKİ VE MALZEMESİNDEKİ DEĞİŞİME BAĞLI DEFORMASYONUN İNCELENMESİ," *researchgate.netN YILDIRIM, S KURTAR, G BEDENLİ, T DAĞ, M ÖZTÜRK, T ÜNLERresearchgate.net*, 2022, Accessed: Feb. 01, 2025. [Online]. Available: https://www.researchgate.net/profile/Tarik-Uenler-2/publication/362072459_INSANSIZ_HAVA_ARACI_KANADINDA_RIB_SAYISINDAKI_VE_MALZEMESINDEKI_DEGISIME_BAGLI_DEFORMASYONUN_INCELENMESI/links/62d557698fb4871182264335/INSANSIZ-HAVA-ARACI-KANADINDA-RIB-SAYISINDAKI-VE-MALZEMESINDEKI-DEGISIME-BAGLI-DEFORMASYONUN-INCELENMESI.pdf

[3] A. Cankurt, "OPTIMUM DESIGN OF COMPOSITE STIFFENED PANELS WITH INSTABILITY CONSIDERATIONS A THESIS SUBMITTED TO THE GRADUATE SCHOOL OF NATURAL AND APPLIED SCIENCES OF MIDDLE EAST TECHNICAL UNIVERSITY," 2013.

[4] T. Dag, N. Yildirim, G. Senturk, M. Durmazoglu, S. Yildirim, and M. Uyaner, "Virtual Investigation on the Response of Glare to Low Velocity Impact," *Proceedings of 10th International Conference on Recent Advances in Air and Space Technologies, RAST 2023*, 2023, doi: 10.1109/RAST57548.2023.10198016.

[5] M. Kazemi and G. Verchery, "Design of composite laminated plates for maximum buckling load with stiffness and elastic modulus constraints," *Compos Struct*, vol. 148, pp. 27–38, Jul. 2016, doi: 10.1016/J.COMPSTRUCT.2016.03.051.

[6] K. Tekkanat and Ö. Keleş, "Uçak Kanadının Entegre Güçlendirilmiş Panel Yapıları Kullanılarak Yapısal Tasarımı **," *European Journal of Science and Technology Special Issue*, pp. 64–71, 2020, doi: 10.31590/ejosat.araconf9.

[7] L. Lanzi and V. Giavotto, "Post-buckling optimization of composite stiffened panels: Computations and experiments," *Compos Struct*, vol. 73, no. 2, pp. 208–220, May 2006, doi: 10.1016/J.COMPSTRUCT.2005.11.047.

[8] K. Kumar, A. Kumar, M. Kumar, and A. Info, "Design and analysis of composite overwrapped pressure vessel with analysis of various overwrapping pattern," *Article in International Journal for Modern Trends in Science and Technology*, vol. 8, no. 06, pp. 27–32, 2022, doi: 10.46501/IJMTST0806005.

[9] W. Miller, C. Smith, F. Scarpa, K. E.-C. S. and, and undefined 2010, "Flatwise buckling optimization of hexachiral and tetrachiral honeycombs," *ElsevierW Miller, CW Smith, F Scarpa, KE EvansComposites Science and Technology, 2010•Elsevier*, 2009, doi: 10.1016/j.compscitech.2009.10.022.

[10] N. Bouslama□, A. Maslouhi, and P. Masson, "Experimental and numerical investigation of damage evolution in carbon fiber reinforced polymer stiffened panel in post-buckling regime," *Article Journal of Composite Materials*, vol. 2022, no. 15, pp. 2455–2470, 2019, doi: 10.1177/00219983221096888.

[11] M. Petyt, *Introduction to finite element vibration analysis*. 2010. Accessed: Jan. 23, 2024. [Online]. Available: https://books.google.com/books?hl=tr&lr=&id=N71ACcE-dXwC&oi=fnd&pg=PR11&dq=Petyt,+Maurice.+Introduction+to+finite+element+vibration+analysis.+Cambridge+university+press,+2010&ots=egbGd8ZttB&sig=AeXoc_pQM42hmRvsoPr80zLxnSs

[12] O. Das, H. Ozturk, and C. Gonenli, "Dynamic and Buckling Analysis of the Laminated Composite Curved Plate Frame Structures," *AKU J. Sci. Eng*, vol. 23, pp. 228–246, 2023, doi: 10.35414/akufemubid.1071280.

[13] E. Altunsaray, I. B.-T. Dergi, and undefined 2021, "Buckling Analysis of Symmetrically Laminated Rectangular Thin Plates under Biaxial Compression," *dergipark.org.trE Altunsaray, I BayerTeknik Dergi, 2021•dergipark.org.tr*, vol. 32, no. 6, pp. 2021–11287, Nov. 2021, doi: 10.18400/tekderg.606620.

[14] H. Ersoy, B. Akgöz, and Ö. Civalek, "Static analysis of laminated conical shells by Discrete Singular Convolution (DSC) approach," *KSCE Journal of Civil Engineering*, vol. 18, no. 5, pp. 1455–1463, 2014, doi: 10.1007/S12205-014-0314-8.

[15] D. Quinn, A. Murphy, W. Mcewan, and F. Lemaitre, "Stiffened panel stability behaviour and performance gains with plate prismatic sub-stiffening," *Thin Walled Structures*, vol. 47, pp. 1457–1468, 2009, doi: 10.1016/j.tws.2009.07.004.

[16] A. Ö. Çiftçioğlu, "Kısıtlı Mühendislik Problemlerinin Karşılaştırmalı Ağırlık ve Maliyet Optimizasyonu," *dergipark.org.trAÖ ÇiftçioğluMühendis ve Makina, 2021•dergipark.org.tr*, Accessed: Jan. 23, 2024. [Online]. Available: https://dergipark.org.tr/en/pub/muhendismakina/article/1034211

[17] O. Halis TOTUK, S. Mıstıkoğlu, and M. A. Güvenç, "Design, Optimization, Simulation, and Implementation of a 3D Printed Soft Robotic Peristaltic Pump," 2023, doi: 10.21203/rs.3.rs-3182693/v1.

[18] M. Ali Güvenç, M. Çakır, and S. Mistikoglu, "Experimental Study on Optimization of Cutting Parameters by Using Taguchi Method for Tool Vibration and Surface Roughness in Dry Turning of AA6013," 2019, Accessed: Jan. 23, 2024. [Online]. Available: https://www.researchgate.net/publication/336251906

[19] M. Fakoor, S. M. N. Ghoreishi, and M. Aminjafari, "Multi-objective Optimization of Buckling Load for a Laminated Composite Plate by Coupling Genetic Algorithm and FEM," 2019.

[20] X. Chen, M. Li, N. An, and J. Zhou, "Maximizing buckling load of metabeams via combinatorial optimization of microstructures," *Modern Physics Letters B*, vol. 37, no. 23, Aug. 2023, doi: 10.1142/S021798492350077X.

[21] Z. Yang, Y. Cao, J. Liu, Z. ; Yang, Y. ; Cao, and J. A. Liu, "A buckling analysis and optimization method for a variable stiffness cylindrical pressure shell of AUV," *mdpi.comZ Yang, Y Cao, J LiuJournal of Marine Science and Engineering, 2021•mdpi.com*, 2021, doi: 10.3390/jmse9060637.